Elsevier Editorial System(tm) for Biomaterials
Manuscript Draft

Manuscript Number:

Title: Effects of the Nanostructure of Dendrimer/DNA Complexes on their Endocytosis and Gene Expression

Article Type: FLA Original Research

Section/Category: Biomaterials & Gene Transfer

Keywords: nonviral vector; gene therapy; synchrotron small angle X-ray scattering; cellular uptake; transfection efficiency

Corresponding Author: Dr. Hsing-Wen Sung,

Corresponding Author's Institution: National Tsing Hua University

First Author: Shu-Fen Peng

Order of Authors: Shu-Fen Peng; Chun-Jen Su; Ming-Cheng Wei; Chun-Yu Chen; Zi-Xian Liao; Po-Wei Lee; Hsin-Lung Chen; Hsing-Wen Sung

Abstract: Cationic dendrimers constitute a potential nonviral vector for gene therapy due to their ability of forming electrostatic complexes with DNA (dendriplexes). However, the supramolecular structure of dendriplexes and its impact on the cellular uptake and gene transfection remain largely unknown. Using synchrotron small angle X-ray scattering, here we show that DNA in complexes with poly(amidoamine) (PAMAM) G4 dendrimers exhibited three distinct packaging states modulated by the degree of their protonation (dp). Our structure characterization suggests that the nanostructure of DNA in dendriplexes transformed from square-packed straightened chains (dp/0.1) to hexagonally-packed superhelices (dp/0.3) and eventually to a beads-on-string configuration (dp/0.6 and dp/0.9). The transfection efficiency in HT1080 cells significantly enhanced when the dp value was increased from 0.1 to 0.3. This enhancement was due to a higher positive surface charge of dendriplexes formed at higher dp, which facilitated adherence of test dendriplexes to the negatively charged cell membranes for the subsequent endocytosis. Although the surface charge of dendriplexes still increased accordingly, further increase of the dendrimer dp value to 0.9 reduced the transfection efficiency. This unexpected suppression of transfection may be attributed to the wrapping of DNA around dendrimers that frustrates the interaction between dendrimer and cholesterol in the membrane raft via the caveola-mediated endocytosis. These results can be used for the rational design of dendrimer-based gene delivery devices.

AUTHOR DECLARATION

We the undersigned declare that this manuscript is original, has not been published before and is not currently being considered for publication elsewhere.

We wish to draw the attention of the Editor to the following facts which may be considered as potential conflicts of interest and to significant financial contributions to this work. [OR]
We wish to confirm that there are no known conflicts of interest associated with this publication and there has been no significant financial support for this work that could have influenced its outcome.

We confirm that the manuscript has been read and approved by all named authors and that there are no other persons who satisfied the criteria for authorship but are not listed. We further confirm that the order of authors listed in the manuscript has been approved by all of us.

We confirm that we have given due consideration to the protection of intellectual property associated with this work and that there are no impediments to publication, including the timing of publication, with respect to intellectual property. In so doing we confirm that we have followed the regulations of our institutions concerning intellectual property.

We understand that the Corresponding Author is the sole contact for the Editorial process (including Editorial Manager and direct communications with the office). He/she is responsible for communicating with the other authors about progress, submissions of revisions and final approval of proofs. We confirm that we have provided a current, correct email address which is accessible by the Corresponding Author and which has been configured to accept email from biomaterials@online.bc.

Signed by all authors as follows:

[LIST AUTHORS AND DATED SIGNATURES ALONGSIDE]

Shu-Fen Peng Shu-Fen Peng

Chun-Jen Su Chun-Jen Su

Ming-Cheng Wei Ming-Cheng Wei

Chun-Yu Chen Chun-Yu Chen 2/8/2010

Po-Wei Lee Po-Wei Lee

Zi-Xian Liao Zi-Xian Liao 2/8/2010

Hsin-Lung Chen H L Chen 2/8/2010

Hsing-Wen Sung Hsing-Wen Sung 2/8/2010

February 10, 2010

Professor D. F. Williams
Editor-in-Chief, Biomaterials

Dear Professor Williams:

Attached please find a manuscript entitled "*Effects of the nanostructure of dendrimer/DNA complexes on their endocytosis and gene expression*". The manuscript is intended to be published in *Biomaterials*. It has been solely submitted to *Biomaterials* and that it is not concurrently under consideration for publication in any other journals.

Cationic dendrimers constitute a potential nonviral vector for gene therapy due to their ability of forming electrostatic complexes with DNA (dendriplexes). However, the supramolecular structure of dendriplexes and its impact on the cellular uptake and gene transfection remain largely unknown. In this study, we have revealed how the degree of protonation (or charge density) of cationic dendrimers modulates the DNA packaging state and forms complexes with distinct nanostructures and their effects on cellular uptake and transfection efficiency. The results obtained in the study can be used to fine-tune the dendriplex nanostructure for the rational design of gene carriers.

We value you and the reviewers' suggestions and comments. Thank you in advance for arranging the review process for our manuscript.

Sincerely yours,

Hsing-Wen Sung, Ph.D.
Professor
Department of Chemical Engineering
National Tsing Hua University
Hsinchu, Taiwan 30013
Phone: +886-3-574-2504
Fax: +886-3-572-6832
Email: hwsung@che.nthu.edu.tw

*Title Page

Effects of the Nanostructure of Dendrimer/DNA Complexes on their Endocytosis and Gene Expression

Short Title: Dendrimer/DNA Complexes for Gene Delivery

Shu-Fen Peng[1]†, Chun-Jen Su[2]†, Ming-Cheng Wei[1], Chun-Yu Chen[1], Zi-Xian Liao[1], Po-Wei Lee[1], Hsin-Lung Chen[1]*, Hsing-Wen Sung[1]*

[1] Department of Chemical Engineering, National Tsing Hua University, Hsinchu, Taiwan, R.O.C.

[2] National Synchrotron Radiation Research Center, Hsinchu, Taiwan, R.O.C.

***Correspondence to:**

Hsing-Wen Sung, PhD

Professor

Department of Chemical Engineering

National Tsing Hua University

Hsinchu, Taiwan 30013

Tel: 886-3-574-2504

Fax: 886-3-572-6832

E-mail: hwsung@che.nthu.edu.tw

†The first two authors (Shu-Fen Peng and Chun-Jen Su) contributed equally to this work.

*To whom correspondence should be addressed: hwsung@che.nthu.edu.tw (H.W. Sung) and hlchen@che.nthu.edu.tw (H.L. Chen).

Abstract

Cationic dendrimers constitute a potential nonviral vector for gene therapy due to their ability of forming electrostatic complexes with DNA (dendriplexes). However, the supramolecular structure of dendriplexes and its impact on the cellular uptake and gene transfection remain largely unknown. Using synchrotron small angle X-ray scattering, here we show that DNA in complexes with poly(amidoamine) (PAMAM) G4 dendrimers exhibited three distinct packaging states modulated by the degree of their protonation (dp). Our structure characterization suggests that the nanostructure of DNA in dendriplexes transformed from square-packed straightened chains (dp/0.1) to hexagonally-packed superhelices (dp/0.3) and eventually to a beads-on-string configuration (dp/0.6 and dp/0.9). The transfection efficiency in HT1080 cells significantly enhanced when the dp value was increased from 0.1 to 0.3. This enhancement was due to a higher positive surface charge of dendriplexes formed at higher dp, which facilitated adherence of test dendriplexes to the negatively charged cell membranes for the subsequent endocytosis. Although the surface charge of dendriplexes still increased accordingly, further increase of the dendrimer dp value to 0.9 reduced the transfection efficiency. This unexpected suppression of transfection may be attributed to the wrapping of DNA around dendrimers that frustrates the interaction between dendrimer and cholesterol in the membrane raft via the caveola-mediated endocytosis. These results can be used for the rational design of dendrimer-based gene delivery devices.

Keywords: nonviral vector; gene therapy; synchrotron small angle X-ray scattering; cellular uptake; transfection efficiency

1. Introduction

Numerous materials have been studied as potential vectors for gene delivery with varying results [1]. Dendrimers constitute a unique class of hyperbranched macromolecules composed of layers of monomer units radiating from a central core; each complete grafting cycle is called a generation [2,3]. Although dendrimers are less efficient than viral vectors, they have the potential for use in gene therapy and other therapeutic applications due to their safety and lack of immunogenicity [4]. Because of its relatively high transfection efficiency, polyamidoamine (PAMAM) is the most commonly used dendrimers for gene delivery [5]. The amine groups of PAMAM dendrimers can be positively charged through proton transfer in acidic aqueous media. PAMAM dendrimers and DNA form complexes via electrostatic interactions between their protonated amine groups and the negatively charged phosphate groups of nucleic acids [6].

Dendrimers are reported to be internalized into cells by endocytosis [7]. The surface charge of dendrimers may influence their cellular uptake and subsequent transfection efficiency [8]. In this study, we prepared different degrees of protonation (dp, i.e., the number fraction of protonated amine groups) of PAMAM dendrimers and then complex with DNA to form dendriplexes in distinct nanostructures. Understanding the nanostructures of dendriplexes and their effects on the endocytosis and transfection efficiency is essential for the rational design of dendrimer-based gene delivery devices.

The size and zeta potential (surface charge) of the prepared dendriplexes together with their morphology and internal structures were examined by dynamic light scattering (DLS), transmission electron microscopy (TEM) and small angle X-ray scattering (SAXS), respectively. The potential of transfection efficiency of test dendriplexes was evaluated by luminance spectrometry and flow cytometry, while their internalization effectiveness was examined using a confocal laser scanning microscope (CLSM) and a flow cytometer.

2. Materials and Methods

2.1. Plasmid DNA

The plasmid DNAs used in the study were pEGFP-N2 (4.7 kb, coding an enhanced green fluorescence protein reporter gene, Clontech, Palo Alto, CA, USA) and pGL4.13 (4.6 kb, coding a firefly luciferase reporter gene, Promega, Madison, WI, USA). pEGFP-N2 and pGL4.13 were amplified using DH5α and purified by Qiagen Plasmid Mega Kit (Valencia, CA, USA) according to the manufacturer's instructions. The purity of plasmids was analyzed by gel electrophoresis (0.8% agarose), while their concentration was measured by UV absorption at 260 nm (Jasco, Tokyo, Japan). pEGFP-N2 and pGL4.13 were linearized using *Eco*O109I and *Bam*HI (New England Biolabs, Ipswich, MA, USA), respectively, and subsequently purified by Gene-Spin^{TM} 1-4-3 DNA Purification Kit-V^{3} (Protech Technology Enterprise, Taipei, Taiwan).

2.2. Preparation of test dendriplexes

PAMAM G4 dendrimers with a diaminobutane core in methanol solution were acquired from Dendritic Nanotechnologies (Mount Pleasant, MI, USA). After thoroughly drying, the solid was redissolved in distilled water to produce a 0.2% (w/v) stock solution [6]. The solutions were stored at 4°C until use. Subsequently, four different dp values (0.1, 0.3, 0.6 and 0.9) of aqueous dendrimers were prepared by adding predetermined amounts of 0.1*N* HCl. For the preparation of PAMAM/DNA dendriplexes suspension (700 μl) in distinct nanostructures, 32.5 μg of linear pEGFP-N2 (or pGL4.13) was individually added to 222.5 μg of aqueous dendrimers with different dp values and then thoroughly mixed for 30–60 s using a vortexer and left for at least 1 h at room temperature. The molar ratio of the amine groups (N) of dendrimers to the phosphate groups (P) of DNA was 1, 3, 6, 10, 15 or 20.

2.3. Characterization of test dendriplexes

The loading efficiency of DNA in each studied group was measured by the PicoGreen assay [9,10]. Briefly, 200 μl of the PicoGreen reagent (diluted 200-fold, Molecular Probes, Carlsbad, CA, USA) was mixed with the same volume of a blank solution (TE buffer, 10*mM* Tris-Cl, pH 7.5, 1*mM* EDTA) or dendriplex solutions prepared at various N/P ratios. After 2 min incubation, each solution was added to 1.6 ml of TE buffer in a test tube and then analyzed using a FL-2500 Fluorescence Spectrofluorometer (Hitachi, Japan). Results were

represented as relative fluorescence (%) to DNA control.

The retardation of DNA in dendriplexes prepared at different dp values was evaluated by electrophoresis. The size and zeta potential of test dendriplexes were investigated using DLS (Zetasizer 3000HS, Malvern Instruments Ltd., Worcestershire, UK). The morphology of test dendriplexes was examined by TEM (JEOL, Tokyo, Japan) [11].

2.4. SAXS experiments

The internal structure of test dendriplexes was probed by SAXS. Aqueous suspensions of dendriplexes prepared using DNA and dendrimers with dp values of 0.1, 0.3, 0.6 and 0.9 were individually introduced into the sample cell comprising two ultralene windows for SAXS measurements. The SAXS experiments were performed at room temperature using Beamline BL17A1 at the National Synchrotron Radiation Research Center (NSRRC), Hsin-Chu, Taiwan. The wavelength (λ) of the X-ray was 1.333 Å and a two-dimensional MAR image plate with 100 x 100 μm^2 pixel resolution was used to collect the scattering intensity data. The sample-to-detector distance and flat-field correction were calibrated by the mixture of silver behenate and Si powders. The intensity profile was output as the plot of the scattering intensity (I) vs. the scattering vector, $q = 4\pi/\lambda \sin(\theta/2)$ (θ = scattering angle) [12].

2.5. In vitro transfection

HT1080 (human fibrosarcoma) cells were cultured in a supplemented cell medium (Dulbecco's Modified Eagle's Medium, DMEM) with 1% penicillin-streptomycin and 10% fetal bovine serum (FBS). Cells were seeded on 12-well plates at 2×10^5 cells/well overnight and then transfected at 50–80% confluency [13]. Prior to transfection, the media were removed and cells were rinsed twice with transfection media (DMEM without FBS). Subsequently, a dendriplex suspension containing DNA originally prepared in pure water was applied to each well for transfection. Cells were replenished with 1.1 ml transfection media containing test dendriplexes solution (5 μg DNA) or naked DNA (5 μg DNA).

At 4 h post transfection, the transfection media containing dendriplexes were removed; the cells rinsed three times with transfection media and refilled with FBS-containing media

until analysis at 24 h after transfection. Cells were then observed under a fluorescence microscope (Carl Zeiss Optical, Berlin, Germany) to monitor any morphological changes and to obtain an estimate of the transfection efficiency. At 4 h after transfection, EGFP-positive cells were clearly observed for all studied groups; with time progressing, the expression of EGFP increased significantly. At 24 h post transfection, the number of EGFP-positive cells was quantified using flow cytometry. Cells transfected with Lipofectamine^{TM} 2000 (Invitrogen, Carlsbad, CA, USA) were used as a positive control and those without any treatment were used as a negative control.

2.6. Percentage of cells transfected

The percentage of cells transfected was quantitatively assessed at 24 h after transfection by flow cytometry. Cells were detached by 0.05% collagenase. Cell suspensions were then transferred to microtubes, fixed by 4% paraformaldehyde and determined the percentage of cells transfected by a flow cytometer (Beckman Coulter, Fullerton, CA, USA) equipped with a 488 nm argon laser for excitation. For each sample, 10,000 events were collected and fluorescence was detected. Signals were amplified in logarithmic mode for fluorescence to determine the EGFP positive events by a standard gating technique. The percentage of positive events was calculated as the events within the gate divided by the total number of events, excluding cell debris.

2.7. Gene expression level

The gene expression levels of cells were assayed by quantifying the expressions of luciferase. Cells were plated on 24-well plates (1×10^5 cells/well) and transfected as described above with the exception that 2 μg pGL4.13 was used. The cells transfected were lysed by 100 μl of passive lysis buffer (Promega). The cell lysate was transferred into a 1.5-ml microtube, while the cell debris was separated by centrifugation (14,000 rpm, 5 min). Subsequently, a 100 μl of the luciferase assay reagent (Promega) was added to a 20 μl of the supernatant and the relative luminescence of the sample was determined by a microplate luminometer (Berthold Technologies, Bad Wildbad, Germany) and normalized to the total cell protein concentration by the Bradford method.

2.8. MTT assay

The cytotoxicity of test dendriplexes was evaluated *in vitro* using the MTT assay [13]. HT1080 cells were seeded on 24-well plates at a density of 1×10^5 cells/well, allowed to adhere overnight and transfected by test dendriplexes containing 2 μg DNA. After 4 h, test samples were aspirated and cells were replenished with a fresh growth medium and incubated for another 20 h. Subsequently, cells were incubated in a growth medium containing 1 mg/ml MTT reagent for an additional 4 h; each medium was then removed prior to the addition of a 500 μl of dimethyl sulfoxide to ensure solubilization of formazan crystals. Finally, the optical density readings were performed using a multiwall scanning spectrophotometer (Dynatech Laboratories, Chantilly, VA, USA) at a wavelength of 570 nm.

2.9. Fluorescent dendriplex preparation, CLSM visualization and flow-cytometry analysis

FITC-labeled dendrimers were synthesized as per the methods described in the literature [14]. To remove the unconjugated FITC, the synthesized FITC-dendrimers were dialyzed in the dark against deionized water and replaced on a daily basis until no fluorescence was detected in the supernatant. The resultant FITC-dendrimers were dried in an oven. FITC-labeled dendriplexes were then prepared as described before to track the internalization of dendriplexes by CLSM (TCS SL, Leica, Germany) and to quantify their cellular uptake by flow cytometry, respectively.

To track the internalization of dendriplexes, cells were seeded on 12-well plates with a sterile glass coverslip at 2×10^5 cells/well and incubated overnight. Subsequently, cells were rinsed twice with transfection media and transfected with FITC-labeled dendriplexes. After incubation for 1 h, test samples were aspirated. Cells were then washed twice with pre-warmed phosphate buffered saline (PBS) before they were fixed in 4% paraformaldehyde. Finally, the fixed cells were examined under a CLSM.

To quantify the cellular uptake of dendriplexes, cells were plated on 12-well plates and transfected with FITC-labeled dendriplexes at a concentration of 5 μg DNA/well for 1 h. After transfection, cells were detached by 0.05% collagenase and transferred to microtubes. Subsequently, cells were resuspended in PBS containing 1*mM* EDTA and fixed in 4%

paraformaldehyde. Finally, the cells were introduced into a flow cytometer equipped with a 488-nm argon laser.

2.10. Endocytosis inhibition

Cells were pre-incubated with the following inhibitors at concentrations which were not toxic to the cells: 10 μg/ml of chlorpromazine [15], 50*nM* wortamannin [16], 200μM Genistein [4,8], 5 μg/ml filipin [4] or 10*mM* MβCD [4]. Following the pre-incubation for 30 min, the inhibitor solutions were removed, and freshly prepared dendriplexes (FITC-labeled) in media containing the same inhibitor concentrations as those mentioned above were individually added and further incubated for 1 h. Subsequently, the cells were washed three times with PBS, collected according to the methods described above and analyzed by flow cytometry.

2.11. Statistical analysis

Comparison between groups was analyzed by the one-tailed Student's *t*-test (SPSS, Chicago, Ill). All data are presented as a mean value with its standard deviation indicated (mean ± SD). Differences were considered to be statistically significant when the *P* values were less than 0.05.

3. Results and Discussion

3.1. Preparation of test dendriplexes and optimization of N/P ratio for transfection study

PAMAM dendrimers and DNA formed dendriplexes via electrostatic interactions, and their constituted compositions for transfection were optimized using EGFP/flow-cytometric analysis of transfected cells. As shown in Fig. 1a, the percentage of transfected cells increased significantly with increasing the N/P ratio of dendriplexes ($P < 0.05$). Among all studied groups, the maximum transfection was found at an N/P ratio of 15/1 or 20/1; however, significant cell toxicity was observed in these two groups. Additionally, a dose-dependent increase in the number of cells transfected was seen (Fig. 1b); but a low cell viability was observed when 10 μg DNA/well was used. Therefore, preparation of test dendriplexes was carried out using an N/P ratio of 10/1 and an amount of 5 μg DNA/well

was used in the subsequent experiments.

3.2. Size and zeta potential of test dendriplexes

As shown in Table 1, the sizes of the dendriplex particles prepared at distinct dp values were in the range of 150 to 165 nm and their zeta potential increased with increasing dp. Fig. 2a displays a representative TEM micrograph of a dendriplex nanoparticle with a dp value of 0.1. As shown, the particle was quite compact and largely spherical in shape. Similar feature was observed for the complexes with other dp values.

3.3. Nanostructure of dendriplexes

SAXS was employed here to probe the internal nanostructure of test dendriplexes. Because the electron density contrast of DNA relative to water is about 2.85 times that of PAMAM dendrimers, the SAXS intensity of the complex is dominated by the partial structure factor associated with DNA-DNA correlation; consequently, the scattering curve mainly yields the information about the spatial organization of DNA within dendriplex particles [17–19].

Fig. 2b shows the SAXS profiles of test dendriplexes formed at different dp values. The scattering profile of dp/0.1 complexes exhibited three lattice peaks with the relative positions of $1:2^{1/2}:4^{1/2}$, showing the formation of a square columnar phase in which the DNA chains arranged in a square lattice [17–19], as schematically illustrated in Fig. 3a. The DNA chains in the square lattice are relatively straightened, and the dendrimer macrocations are accommodated in the interstitial tunnels between DNA.

For dendriplexes with a high dp value of 0.6 or 0.9, the SAXS profiles displayed a strong peak at ca. 2.3 nm^{-1} and a vaguely identified peak at 1.45 or 1.28 nm^{-1}. The feature of the scattering pattern was quite similar to that of the previously reported SAXS profiles of chromatin [20–22], suggesting that the strong electrostatic attraction induced wrapping of DNA around the dendrimer for effective charge matching to yield the chromatin-like "beads-on-string structure" (Fig. 3b). The scattering peak at ca. 2.3 nm^{-1} (q_p) was attributed to the highly regular pitch of the wrapping, while the small peak observed at lower q was considered to be associated with the interparticle distance *d* of the "nucleosome-like"

particles.

The formation of beads-on-string structure in dp/0.6 and dp/0.9 complexes was verified by comparing the observed SAXS profiles with the calculated scattering curve of an open chromatin-like fiber. We first constructed a chromatin-like rod formed by a DNA chain (approximated by a flexible uniform cylinder with the diameter of 2.0 nm) wrapping around a number of dendrimer macrocations (with each approximated by a uniform sphere with the diameter of 4 nm) placing along a fiber axis with the axial interparticle distance *d*. The wrapping was assumed to be tight with a regular pitch length of *P* (Fig. 3b). The scattering profile of such a structure was then calculated by the Debye equation [23]. The solid curve (in red) superposing on the SAXS profile of dp/0.9 dendriplexes was the calculated scattering curve of a chromatin-like fiber composing of 9 nucleosome-like particles placing in sequence with the values of *P* and *d* of 2.9 nm and 4.8 nm, respectively. It can be seen that the assumed beads-on-string model reproduced the basic feature of the observed SAXS profile.

For dp/0.3 dendriplexes, the scattering profile exhibited a primary peak at 1.44 nm^{-1}, a broad peak at 1.97 nm^{-1} and a small peak at 2.5 nm^{-1}. The position ratio 2.5 nm^{-1} peak to the primary peak was about $1:3^{1/2}$, implying that DNA in the dendriplex packed in a hexagonal lattice. The 1.97 nm^{-1} peak was however not prescribed by the higher-order diffraction of the hexagonal lattice. It has been shown in the foregoing analysis of the beads-on-string structure that the twist of DNA into superhelix could give rise to a pitch scattering peak. Therefore, we proposed that the electrostatic attraction with dp/0.3 dendrimer induced a moderate twist of DNA into superhelices packed in a hexagonal lattice and the 1.9 nm^{-1} peak corresponded to pitch scattering, as schematically illustrated in Fig. 3c. This structure is called ‘hexagonally-packed DNA superhelices”.

The structure characterization thus suggests that the structure of DNA in the dendriplexes transformed from square-packed straightened chains (dp/0.1) to hexagonally-packed superhelices (dp/0.3) and eventually to a beads-on-string configuration (dp/0.6 or dp/0.9). This structural transformation was in accord with the increasing

weighting of electrostatic attraction over DNA bending energy with increasing charge density. Due to their similarity in structural configuration for dp/0.6 and dp/0.9 dendriplexes, only the latter one together with dp/0.1 and dp/0.3 complexes were chosen for the rest of the study.

3.4. DNA loading efficiency and agarose gel retardation

The PicoGreen assay was performed to assess the loading efficiencies of DNA in test dendriplexes prepared at different N/P ratios and dp values [24]. PicoGreen reagent, a DNA intercalating dye, is more sensitive than ethidium bromide. The fluorescence of PicoGreen reagent is quenched when anionic DNA is condensed into dendriplexes with cationic dendrimers [10]. As compared with free DNA (Fig. 4a), little fluorescence was detected for the dendriplexes prepared at distinct N/P ratios and dp values, indicating that their DNA loading efficiencies were about the same and approached 100%.

The binding capacity of dendrimers with DNA in dendriplexes prepared at various dp values was evaluated using the gel retardation assay and the results are given in Fig. 4b. As shown, the migration of DNA was retarded completely, suggesting that the prepared dendriplexes were physically stable.

3.5. Percentage of cells transfected and gene expression level

To explore effects of the nanostructure of dendriplexes on the transfection efficiency, cells were treated with test dendriplexes prepared at different dp values. Transfection efficiencies were presented by two numeric indicators: percentage of cells transfected and gene expression level [25]. As shown in Fig. 5a, at 4 h after transfection, EGFP-positive cells were clearly observed for all studied groups; with time progressing, the expression of EGFP increased significantly. At 24 h post transfection, the number of EGFP-positive cells was quantified using flow cytometry. As shown in Fig. 5b, the percentage of cells transfected with dp/0.3 dendriplexes was significantly higher than those treated with dp/0.1 or dp/0.9 dendriplexes ($P < 0.05$).

The gene expression levels of cells were assayed by quantifying the expression of luciferase with a microplate luminometer. As indicated in Fig. 5c, the luciferase gene

expression level for the group transfected by dp/0.3 dendriplexes was significantly greater than those treated with dp/0.1 or dp/0.9 dendriplexes ($P < 0.05$).

3.6. Cytotoxicity

The cytotoxicity of PAMAM dendrimers and their dendriplex counterparts prepared at distinct dp values was evaluated by the MTT assay and the results are given in Fig. 6. As compared to negative control (NC, the group without any treatment) and naked DNA (NK), the viability of cells treated with PAMAM dendrimers or Lipofectamine^{TM} 2000 decreased relatively ($P < 0.05$). Polycations have been used as transfection agents; most of these cationic materials are comparatively cytotoxic [26]. The cytotoxicity of PAMAM dendrimers is known to be generation dependent [7,27]; low-generation dendrimers showed significantly less cytotoxicity than higher-generations [27]. Additionally, the nature and density of charged groups are other factors that determine the toxicity of dendrimers [28]. With DNA encapsulated, the viability of cells treated with dendriplexes prepared at different dp values decreased further, due to their intracellular expression of EGFP. It is known that EGFP protein is toxic to the cells [29].

3.7. Cellular uptake of test dendriplexes

CLSM was used to visualize the cellular uptake of test dendriplexes. In this experiment, FITC-labeled dendrimers were synthesized and employed to prepare test dendriplexes. At 1 h after transfection, accumulation of FITC-labeled dendriplexes was observed in most of the incubated cells in all studied groups (Fig. 7a). The percentage of cells that internalized FITC-labeled dendriplexes and their fluorescence intensity were quantified by flow cytometry. As shown in Fig. 7b, there was no significant difference in the percentage of cells that internalized FITC-labeled dendriplexes among all studied groups ($P > 0.05$). However, the intensity of fluorescence observed in the group treated with dp/0.3 dendriplexes was significantly stronger than those transfected with dp/0.1 or dp/0.9 dendriplexes ($P < 0.05$, Figs. 7c and 7d).

3.8. Effects of endocytotic inhibitors on cellular uptake of dendriplexes

To elucidate differences in the uptake mechanism, the interaction between test

dendriplexes (FITC-labeled) and cell membranes was investigated by treating cells with different chemical inhibitors and then analyzed by flow cytometry. Their counterparts in the absence of inhibitors were used as controls. Chlorpromazine is used as an inhibitor for clathrin-mediated uptake [15,30] and wortmannin is an inhibitor of macropinocytosis [31]. As shown in Fig. 8, treatment with chlorpromazine did not result in an inhibition of uptake of dendriplexes prepared at different dp values ($P > 0.05$), indicating that none of test dendriplexes appeared to be taken up by the clathrin-mediated endocytosis. In contrast, cells treated with wortmannin caused a significant decrease in cellular uptake for all studied groups ($P < 0.05$), indicating that macropinocytosis was involved in the uptake of test dendriplexes.

It was reported that cholesterol and membrane rafts are involved in membrane trafficking [4]. Manunta *et al.* suggested that membrane cholesterol and raft integrity are physiologically relevant for the cellular uptake of dendriplexes via the caveola-mediated pathway [4]. Caveolae are flask-shaped invaginations in the plasma membrane enriched in cholesterol and spingolipids [32]. Genistein, filipin and methyl-β-cyclodextrin (MβCD) are known to inhibit the caveola-mediated endocytosis, each acting by a different mechanism [4,33]. Genistein, a tyrosine kinase inhibitor, is used to block the caveola-mediated endocytosis [4,34,35]. Filipin is an antibiotic that incorporates into lipid membranes and chelates cholesterol; MβCD, a water-soluble cyclic oligomer of glucopyranoside, acts strictly on the cell surface, selectively extracting cholesterol without being incorporated into plasma membrane [4,34,35].

As compared to controls, cells treated with inhibitors (genistein, filipin or MβCD) diminished the percentage of cellular uptake significantly by about 20–50% ($P < 0.05$, Fig. 8). The highest degree of inhibition (about 40–50%) was found for the cells treated with genistein. The group treated with dp/0.3 dendriplexes had the highest degree of suppression among all studied groups ($P < 0.05$). The aforementioned results of uptake assays suggest that both the macropinocytosis and caveola-mediated routes were involved in the internalization of dendriplexes; but the caveola-mediated pathway played a more significant

role (Fig. 9a).

3.9. Effects of the nanostructure of dendriplexes on endocytosis and transfection efficiency

Our *in vitro* transfection study revealed that the transfection efficiency of dendriplexes did not vary monotonically with dedrimer dp but showed a maximum at dp/0.3 (Figs. 5b and 5c). The fact that the cellular uptake given by the amount of dendriplexes internalized into the cells (Figs. 7c and 7d) also followed the same trend, indicating that endocytosis was the key step governing the transfection efficiency. The higher transfection of dp/0.3 dendriplexes compared with dp/0.1 dendriplexes (Figs. 5b and 5c) can be attributed to their higher positive surface charge (Table 1), which facilitated the adherence of test particles to the negatively charged cell membranes and enhance the subsequent endocytosis process.

Although dp/0.9 dendriplexes had a higher surface charge, the interaction between dendrimer and cholesterol (via the caveola-mediated pathway) was frustrated by their beads-on-string structure (Fig. 9b) as the DNA wrapping around the dendrimer tended to shield such an interaction, thus suppressing the cellular uptake and the transfection efficiency. It is interesting to note that even if the total cellular uptake of dp/0.9 dendriplexes was higher than dp/0.1 counterparts (Figs. 7c and 7d), their transfection efficiencies were comparable (Fig. 5b). This may imply that the expression of DNA carried by dp/0.9 dendriplexes involved a higher activation barrier. Such a barrier may be associated with the dewrapping of DNA from the nucleosome-like particles due to the strong electrostatic attraction.

4. Conclusions

In conclusion, we have revealed how the dp value (or charge density) of cationic dendrimers modulates the DNA packaging state and forms complexes with distinct nanostructures and their effects on endocytosis and gene expression. Formation of the beads-on-string structure at higher dendrimer dp values may exert a negative effect on the transfection efficiency of dendriplexes as the DNA wrapping around dendrimers frustrates the dendrimer-cholesterol interaction via the caveola-mediated endocytosis. The results obtained in the study may be used to fine-tune the dendriplex nanostructure for the rational

design of gene carriers.

Acknowledgments

This work was supported by grants from the National Science Council (NSC97-2120-M-007-001 and NSC97-2923-E-007-001), Taiwan, Republic of China. The synchrotron X-ray scattering experiment supported by the NSRRC under Project ID 2007-1-018-4 and 2007-1-018-5 was gratefully acknowledged.

References

[1] Eichman JD, Bielinska AU, Kukowska-Latallo JF, Baker JR. The use of PAMAM dendrimers in the efficient transfer of genetic material into cells. Pharm Sci Technol Today 2000;3:232–245.

[2] Tomaila DA, Naylor AM, Goddard III WA. Starburst dendrimers: Molecular-level control of size, shape, surface chemistry, topology, and flexibility from atoms to macroscopic matter. Angew Chem Int Ed Engl 1990;29:138–175.

[3] Tomaila DA. Birth of a new macromolecular architecture: Dendrimers as quantized building blocks for nanoscale synthetic polymer chemistry. Prog Polym Sci 2005;30:294–324.

[4] Manunta M, Tan PH, Sagoo P, Kashefi K, George AJT. Gene delivery by dendrimers operates via a cholesterol dependent pathway. Nucleic Acids Res 2004;32:2730–2739.

[5] Morille M, Passirani C, Vonarbourg A, Clavreul A, Benoit JP. Progress in developing cationic vectors for non-viral systemic gene therapy against cancer. Biomaterials 2008;29:3477–3496.

[6] Su CJ, Liu YC, Chen HL, Li YC, Lin HK, Liu WL, et al. Two-dimensional densely packed DNA nanostructure derived from DNA complexation with a low-generation poly(amidoamine) dendrimer. Langmuir 2007;23:975–978.

[7] Seib FP, Jones AT, Duncan R. Comparison of the endocytic properties of linear and branched PEIs, and cationic PAMAM dendrimers in B16f10 melanoma cells. J Control Release 2007;117:291–300.

[8] Perumal OP, Inapagolla R, Kannan S, Kannan RM. The effect of surface functionality on cellular trafficking of dendrimers. Biomaterials 2008;29:3469–3476.

[9] Cui Z, Mumper RJ. Chitosan-based nanoparticles for topical genetic immunization. J Control Release 2001;75:409–419.

[10] Kim TI, Baek JU, Zhe BC and Park JS. Arginine-conjugated polypropylenimine dendrimer as a non-toxic and efficient gene delivery carrier. Biomaterials 2007;28:2061–2067.

[11] Adams CWM. Osmium tetroxide and the Marchi method: Reactions with polar and non-polar lipids, protein and polysaccharide. J Histochem Cytochem 1960;8:262–267.

[12] Hsu WL, Li YC, Chen HL, Liou W, Jeng US, Lin HK, et al. Thermally-induced order-order transition of DNA-cationic surfactant complexes. Langmuir 2006;22:7521–7527.

[13] Peng SF, Yang MJ, Su CJ, Chen HL, Lee PW, Wei MC, et al. Effects of incorporation of poly(gamma-glutamic acid) in chitosan/DNA complex nanoparticles on cellular uptake and transfection efficiency. Biomaterials 2009;30:1797–1808.

[14] Choi Y, Thomas T, Kotlyar A, Islam MT, Baker JR. Jr. Synthesis and functional evaluation of DNA-assembled polyamidoamine dendrimer clusters for cancer cell-specific targeting. Chem Biol 2005;12:35–43.

[15] Von Gersdorff K, Sanders NN, Vandenbroucke R, De Smedt SC, Wagner E, Ogris M. The internalization route resulting in successful gene expression depends on both cell line and polyethylenimine polyplex type. Mol Ther 2006;14:745–753.

[16] Araki N, Johnson MT, Swanson JA. A role for phosphoinositide 3-kinase in the completion of macropinocytosis and phagocytosis by macrophages. J Cell Biol 1996;135:1249–1260.

[17] Liu YC, Chen HL, Su CJ, Liu HK, Liu WL, Jeng U. Mesomorphic Complexes of Poly(amidoamine) Dendrimer with DNA. Macromolecules 2005;38:9434–9440.

[18] Su CJ, Chen HL, Wei MC, Peng SF, Sung HW, Ivanov VA. Columnar Mesophases of the Complexes of in DNA with Low-Generation Poly(amido amine) Dendrimers Biomacromolecules 2009;10:773–783.

[19] Evans HM, Ahmad A, Ewert K, Pfohl T, Martin-Herranz A, Bruinsma RF, et al. Structural polymorphism of DNA-dendrimer complexes. Phys Rev Lett 2003;91:075501–1–075501–4.

[20] Baldwin JP, Boseley PG, Bradbury EM. The subunit structure of the eukaryotic chromosome. Nature 1975;253:245–249.

[21] Pardon JF, Worcester DL, Wooley JC, Cotter RI, Lilley DM, Richards RM. The

structure of the chromatin core particle in solution. Nucleic Acids Res 1977;4:3199–3214.

[22] Williams SP, Athey BD, Muglia LJ, Schappe RS, Gough AH, Langmore JP. Chromatin fibers are left-handed double helices with diameter and mass per unit length that depend on linker length. Biophys J 1986;49:233–248.

[23] Debye PA. Physik 1915;46:809–823.

[24] Nam HY, Nam K, Hahn HJ, Kim BH, Lim HJ, Kim HJ, et al. Biodegradable PAMAM ester for enhanced transfection efficiency with low cytotoxicity. Biomaterials 2009;4:665–673.

[25] Ko IK, Ziady A, Lu S, Kwon YJ. Acid-degradable cationic methacrylamide polymerized in the presence of plasmid DNA as tunable non-viral gene carrier. Biomaterials 2008;29:3872–3881.

[26] Slita AV, Kasyanenko NA, Nazarova OV, Gavrilova II, Eropkina EM. DNA-polycation complexes: Effect of polycation structure on physico-chemical and biological properties. J Biotechnol 2007;127:679–693.

[27] Jevprasesphant R, Penny J, Attwood D, McKeown NB, D'Emanuele A. Engineering of dendrimer surfaces to enhance transepithelial transport and reduce cytotoxicity. Pharm Res 2003;20:1543–1550.

[28] Dufès C, Uchegbu IF, Schätzlein AG. Dendrimers in gene delivery. Adv Drug Deliv Rev 2005;57:2177–2202.

[29] Liu HS, Jan MS, Chou CK, Chen PH, Ke NJ. Is green fluorescent protein toxic to the living cells? Biochem Biophys Res Commun 1999;260:712–717.

[30] Medina-Kauwe LK, Xie J, Hamm-Alvarez S. Intracellular trafficking of nonviral vectors. Gene Ther 2005;12:1734–1751.

[31] Araki N, Johnson MT, Swanson JA. A role for phosphoinositide 3-kinase in the completion of macropinocytosis and phagocytosis by macrophages. J Cell Biol 1996;135:1249–1260.

[32] Parton RG, Simons K. The multiple faces of caveolae. Nature Rev Mol Cell Biol

2007;8:185–194.

[33] Zuhorn IS, Kalicharan R, Hoekstra D. Lipoplex-mediated transfection of mammalian cells occurs through the cholesterol-dependent clathrin-mediated pathway of endocytosis. J Biol Chem 2002;277:18021–18028.

[34] Perumal OP, Inapagolla R, Kannan S, Kannan RM. The effect of surface functionality on cellular trafficking of dendrimers. Biomaterials 2008;29:3469–3476.

[35] Rejman J, Bragonzi A, Conese M. Role of clathrin- and caveolae-mediated endocytosis in gene transfer mediated by lipo- and polyplexes. Mol Ther 2005;12:468–474.

Table

Table 1. Sizes and zeta potentials of test dendriplexes prepared at a defined N/P ratio of 10/1 and various dp values (or charge densities, n = 5).

N/P Ratio = 10/1	Size (nm)	Zeta Potential (mV)
dp/0.1 dendriplexes	149.2 ± 1.7	38.9 ± 0.5
dp/0.3 dendriplexes	151.3 ± 1.6	47.8 ± 0.6
dp/0.6 dendriplexes	161.3 ± 1.2	47.3 ± 1.6
dp/0.9 dendriplexes	163.6 ± 2.5	51.1 ± 1.7

Figure Captions

Figure 1. (a) Percentages of cells that were transfected with dendriplexes (dp/0.1)prepared at different N/P ratios, analyzed by flow cytometry (n = 3); (b) percentages of cells that were transfected with dendriplexes prepared at an N/P ratio of 10/1 with different amounts of DNA/well used (N/P=10), analyzed by flow cytometry (n = 3). NC: negative control (the group without any treatment).

Figure 2. (a) A representative TEM micrograph of a dp/0.1 dendriplex nanoparticle; (b) the SAXS profiles of test dendriplexes with the dp values of 0.1, 0.3, 0.6 and 0.9. The arrows mark the observable scattering peaks.

Figure 3. Schematic illustrations of three distinct nanostructures of test dendriplexes formed at different dendrimer dp values. The rods/strings and the balls represent DNA and dendrimer, respectively. (a) square columnar phase formed at dp/0.1; (b) nucleosome-like beads-on-string structure formed at dp/0.6 or dp/0.9; (c) hexagonally-packed DNA superhelices formed at dp/0.3.

Figure 4. (a) Results of the PicoGreen reagent assay of test dendriplexes. Mean $\pm$ SD (n = 3). (b) Gel retardation analyses of test dendriplexes. Samples were run on a 0.8% agarose gel and subsequently stained using ethidium bromide.

Figure 5. Transfection efficiencies of test dendriplexes. (a) EGFP expressions of cells transfected with dendriplexes prepared at an N/P ratio of 10/1 and different dp values for distinct periods. Cells were transfected *in vitro* using dendriplexes prepared at different dp values after 24 h post-transfection. (b) Percentages of cells that were transfected with test dendriplexes prepared at different dp values, analyzed by flow cytometry (n = 3). (c) Normalized luciferase activities of transfected cells that expressed luciferase, analyzed by a microplate luminometer (n = 5). Cells were transfected *in vitro* using dendriplexes prepared at different dp values at 24 h post transfection. NC: negative control (the group without any treatment); LF: Lipofectamine^{TM} 2000.

Figure 6. Relative viability of cells treated with dendriplexes [with (w/) or without (w/o) DNA] prepared at different dp values. Cells were transfected with test samples for 4 h and analyzed for metabolic activity for 24 h later using the MTT assay (n = 5). Relative viabilities were determined relative to untreated control cells. NC: negative control (the group without any treatment); NK: naked DNA; LF: Lipofectamine^{TM} 2000.

Figure 7. Results of CLSM observation and flow-cytometry analysis of the cellular uptake of test dendriplexes. (a) Confocal images of cells transfected with FITC-labeled dendrimer/DNA complexes prepared at different dp values for 1 h. Cell nuclei were stained with propidium iodide (PI). (b) Percentages of cellular uptake of FITC-labeled dendrimer/DNA complexes prepared at different dp values, analyzed by flow cytometry (n = 3). (c) Intracellular uptake and (d) intracellular fluorescence intensities (n = 3) of FITC-labeled dendrimer/DNA complexes prepared at different dp values, determined by flow cytometry. NC: negative control (the group without any treatment).

Figure 8. Effects of inhibitors on the internalization of test dendriplexes (FITC-labeled). Percentages of intracellular uptake of FITC-labeled dendrimer/DNA complexes prepared at different dp values after the cells were treated with distinct chemical inhibitors, determined by flow cytometry (n = 3). Control: the group without any treatment; Chlor: the group treated with chlorpromazine; Wort: the group treated with wortmannin; Geni: the group treated with genistein; Filipin: the group treated with filipin; MβCD: the group treated with methyl-β-cyclodextrin.

Figure 9. Schematic illustrations of potential mechanisms of internalization of test dendriplexes. (a) Schematic illustrations of potential uptake pathways of test dendriplexes with three distinct packaging states. Both the macropinocytosis and caveola-mediated routes were involved in the internalization of dendriplexes; but the caveola-mediated pathway played a more significant role. (b) Schematic illustrations of the interaction of test dendriplexes prepared at different dp values with cell membranes, specifically for the caveola-mediated endocytosis.

Figure 1

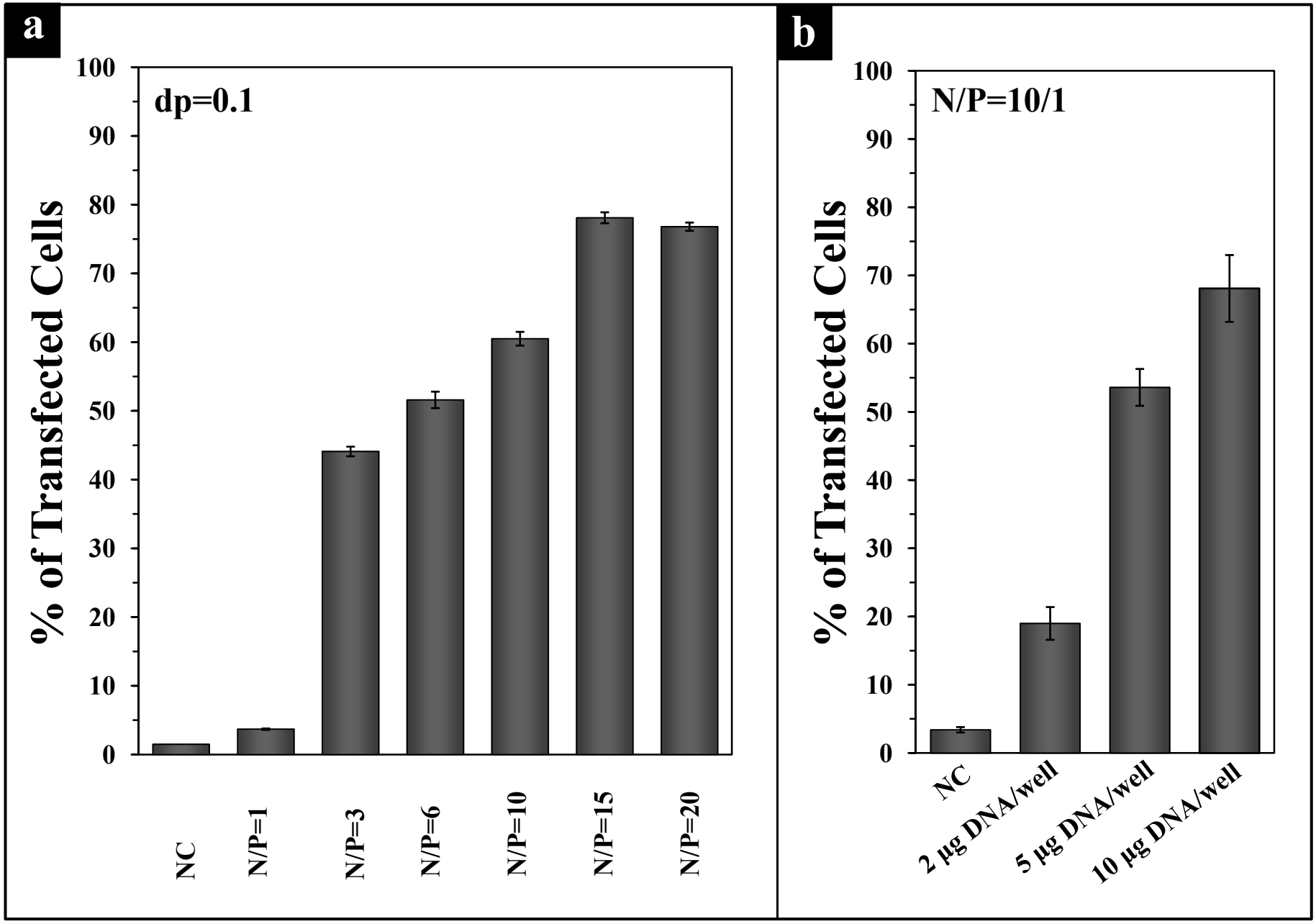
a
dp=0.1
% of Transfected Cells
100
90
80
70
60
50
40
30
20
10
0
NC
N/P=1
N/P=3
N/P=6
N/P=10
N/P=15
N/P=20
b
N/P=10/1
% of Transfected Cells
NC
2 μg DNA/well
5 μg DNA/well
10 μg DNA/well

Figure 2

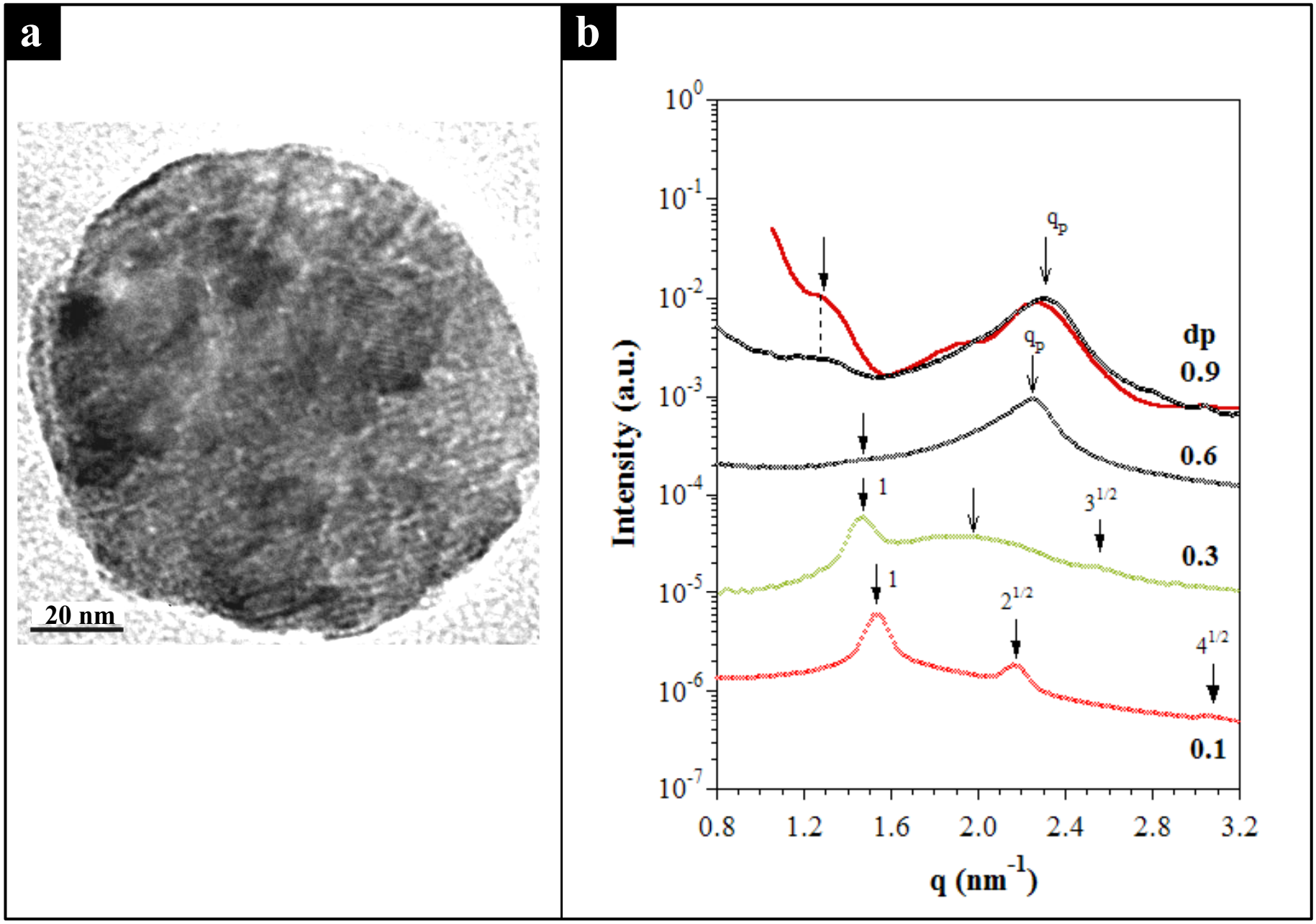
a
20 nm
b
Intensity (a.u.)
q (nm^{-1})
10^{0}
10^{-1}
10^{-2}
10^{-3}
10^{-4}
10^{-5}
10^{-6}
10^{-7}
0.8
1.2
1.6
2.0
2.4
2.8
3.2
q_p
q_p
dp
0.9
0.6
1
$3^{1/2}$
0.3
1
$2^{1/2}$
$4^{1/2}$
0.1

Figure 3

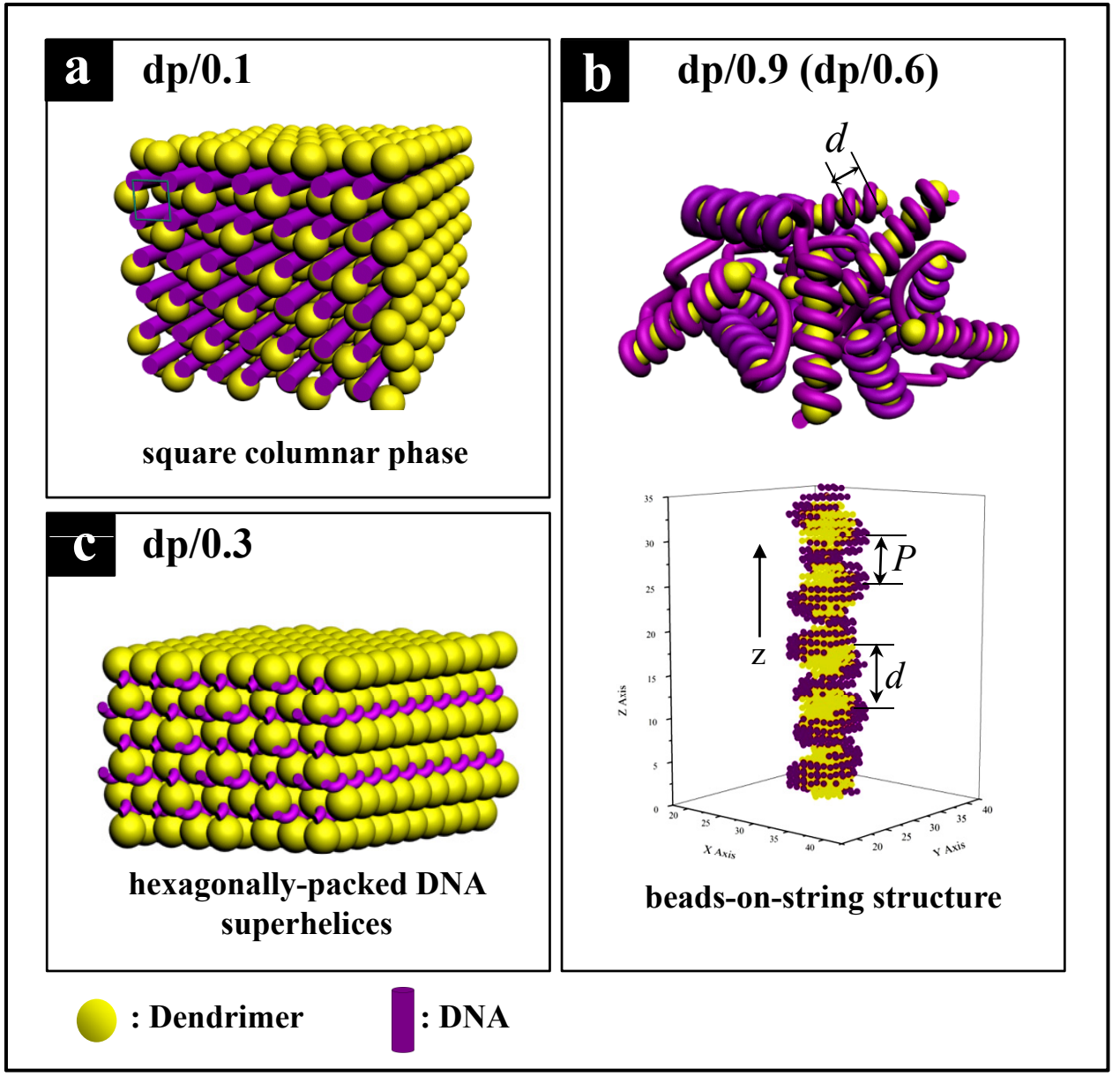
a
dp/0.1
square columnar phase
b
dp/0.9 (dp/0.6)
d
P
z
d
Z Axis
X Axis
Y Axis
beads-on-string structure
c
dp/0.3
hexagonally-packed DNA superhelices
: Dendrimer
: DNA

Figure 4

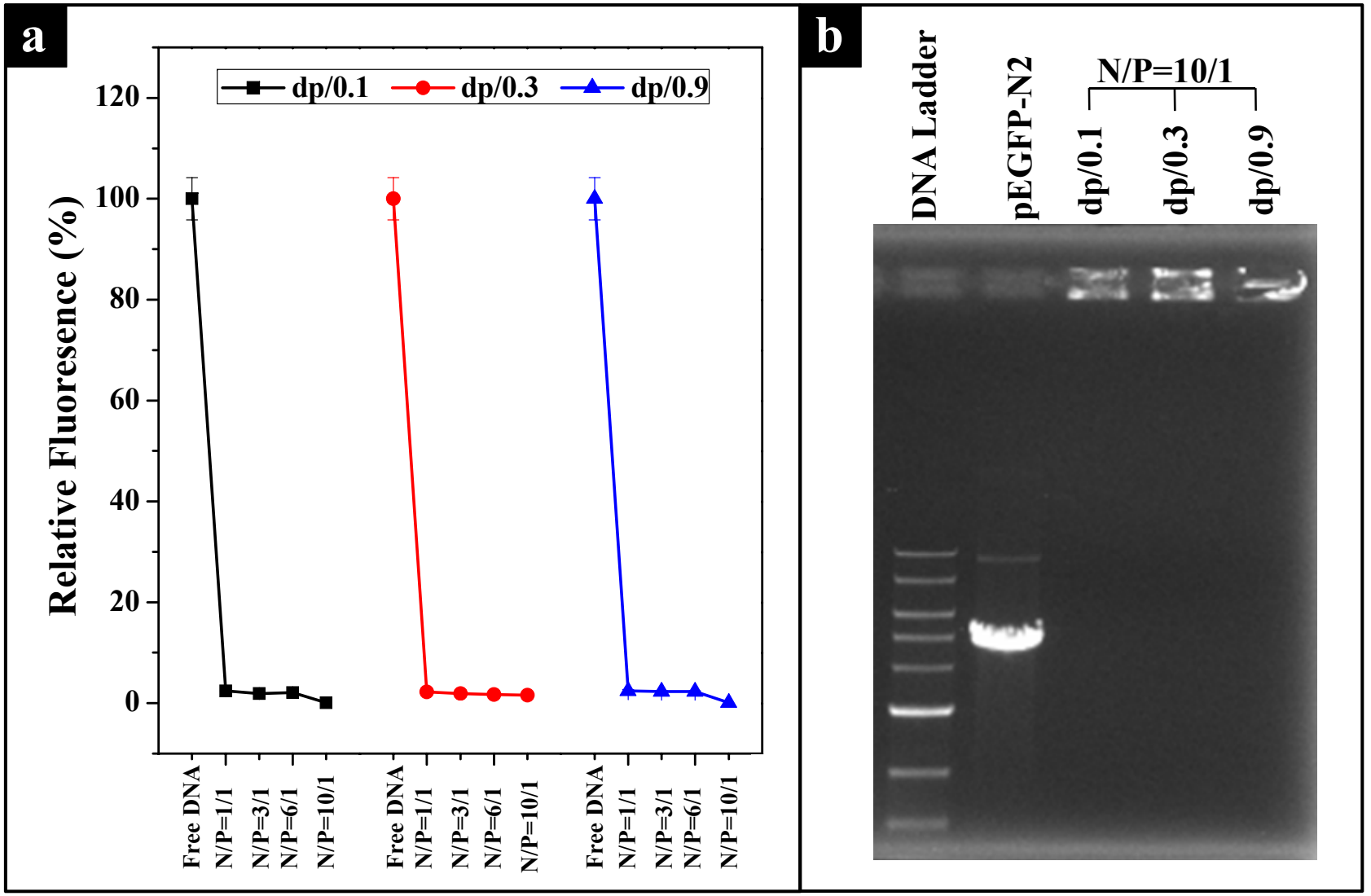
a
dp/0.1
dp/0.3
dp/0.9
Relative Fluoresence (%)
120
100
80
60
40
20
0
Free DNA
N/P=1/1
N/P=3/1
N/P=6/1
N/P=10/1
Free DNA
N/P=1/1
N/P=3/1
N/P=6/1
N/P=10/1
Free DNA
N/P=1/1
N/P=3/1
N/P=6/1
N/P=10/1
b
DNA Ladder
pEGFP-N2
N/P=10/1
dp/0.1
dp/0.3
dp/0.9

Figure 5a

Figure 5

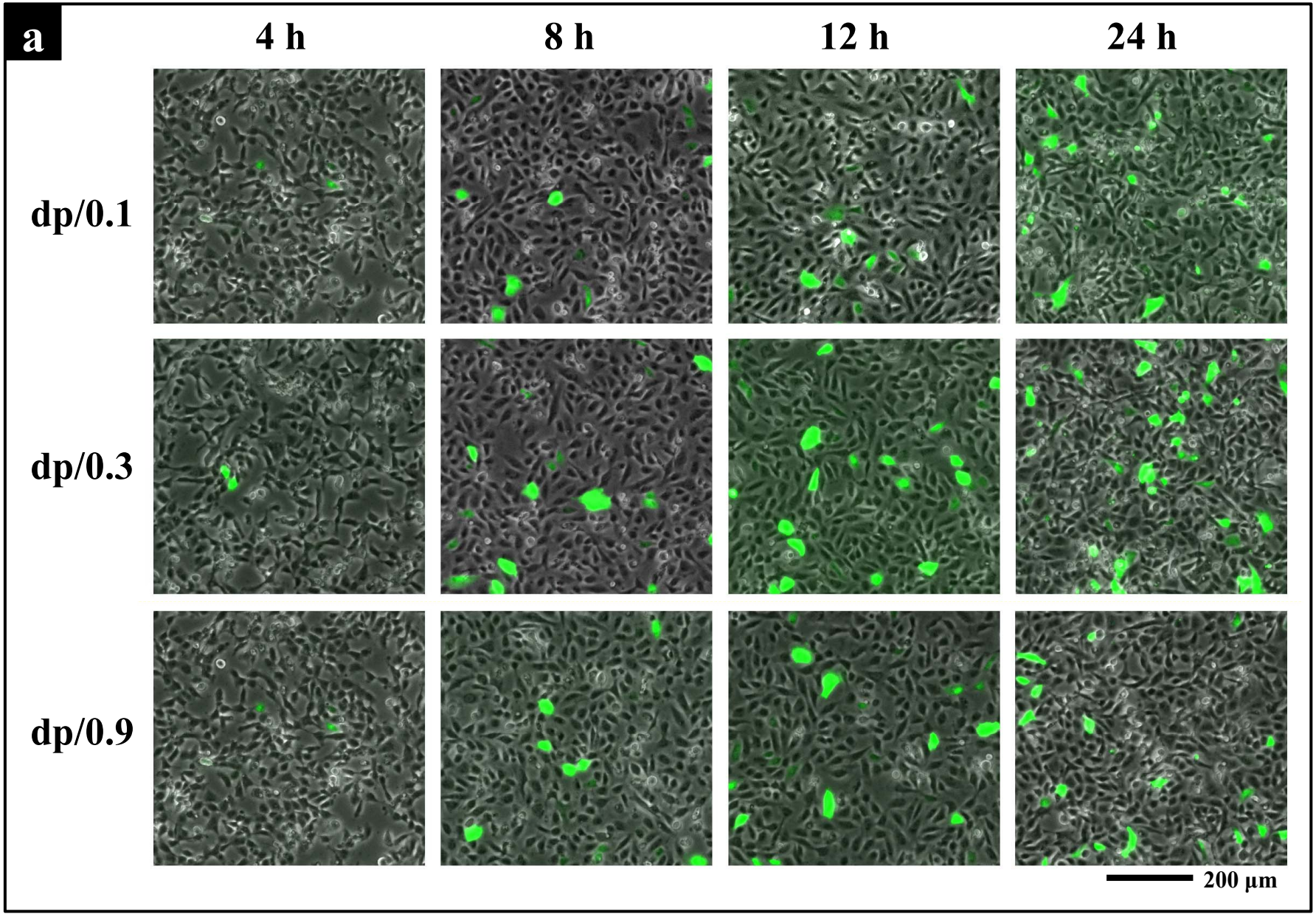

Figure 5b

Figure 5

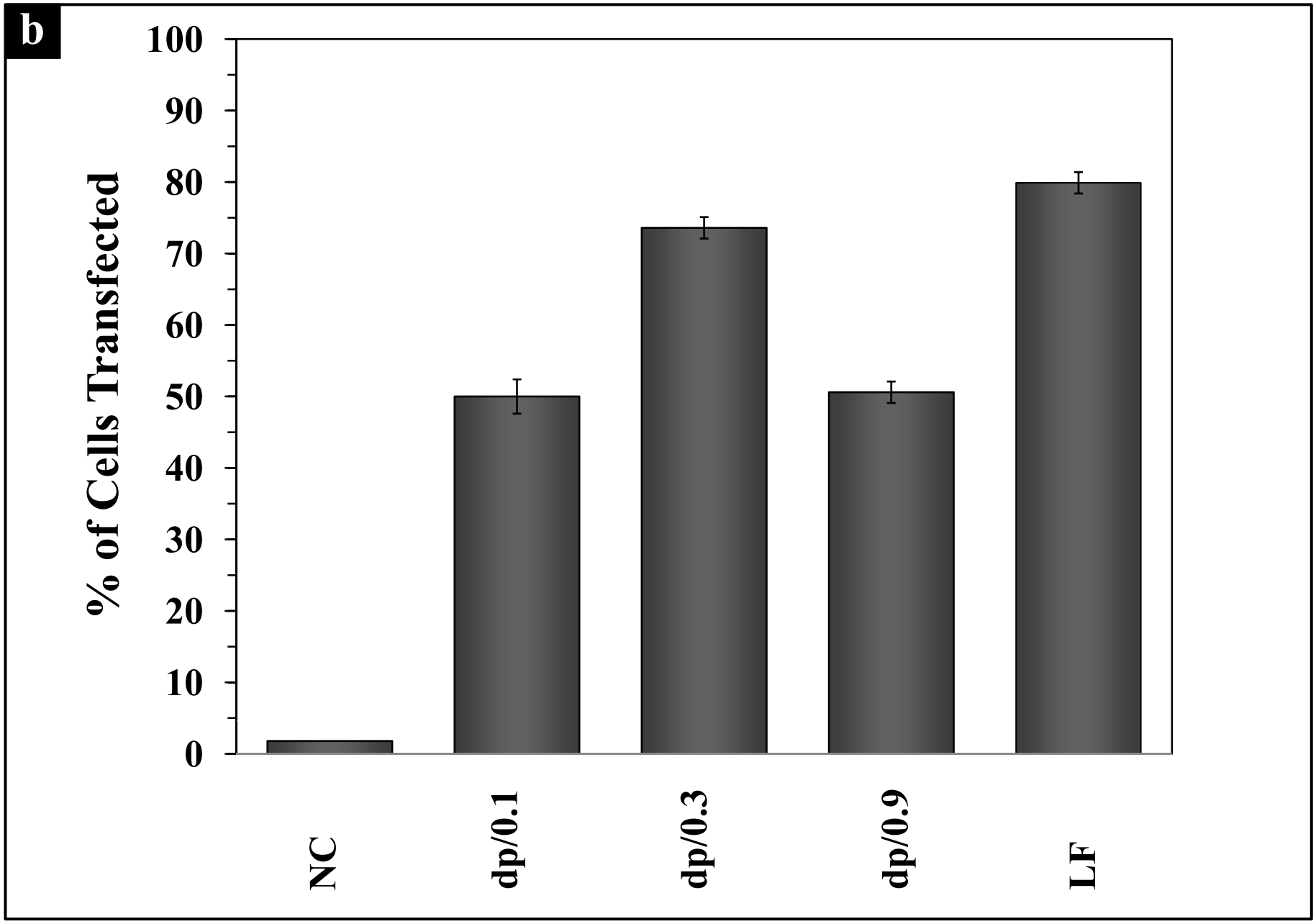

Figure 5c

Figure 5

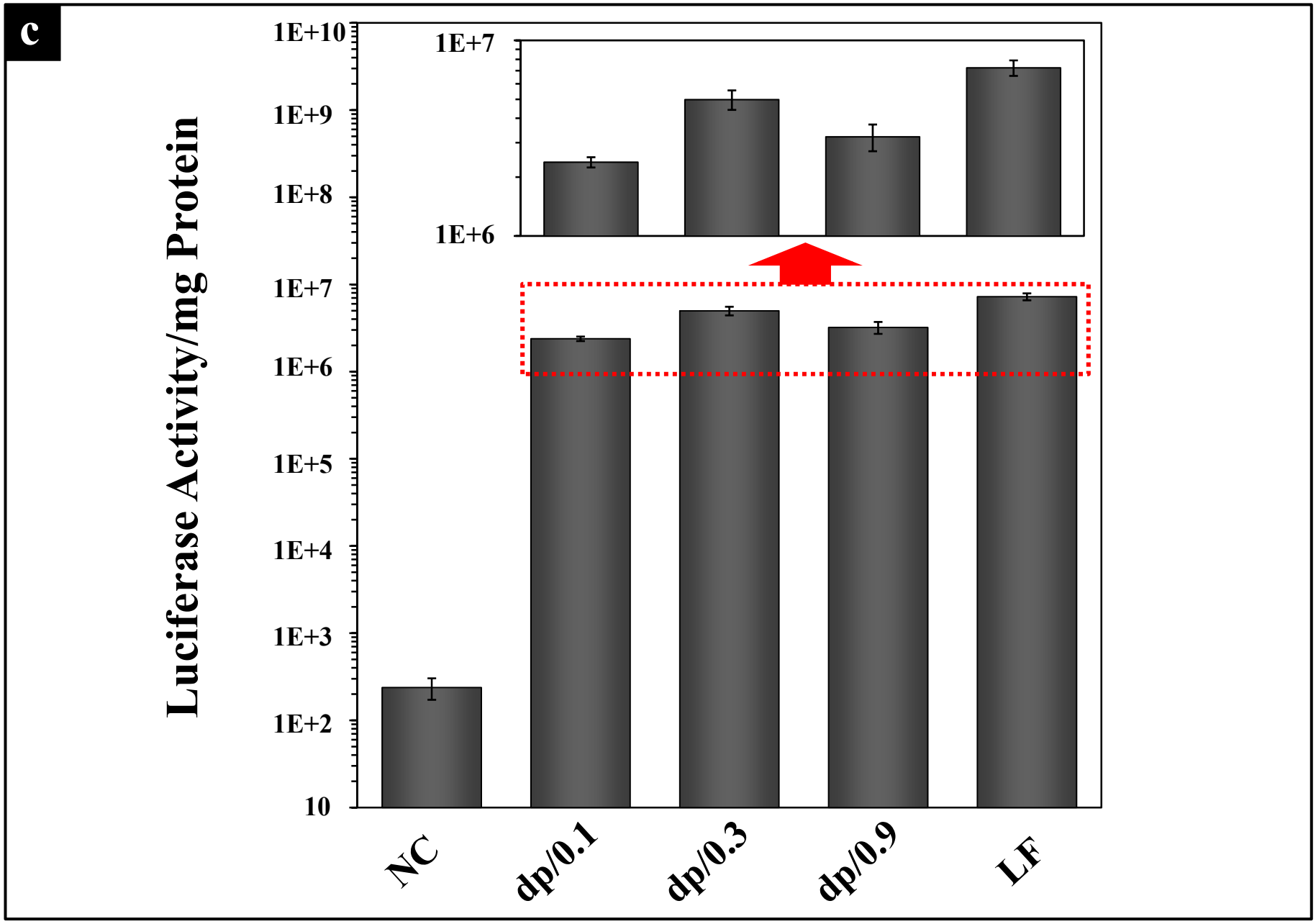

Figure 6

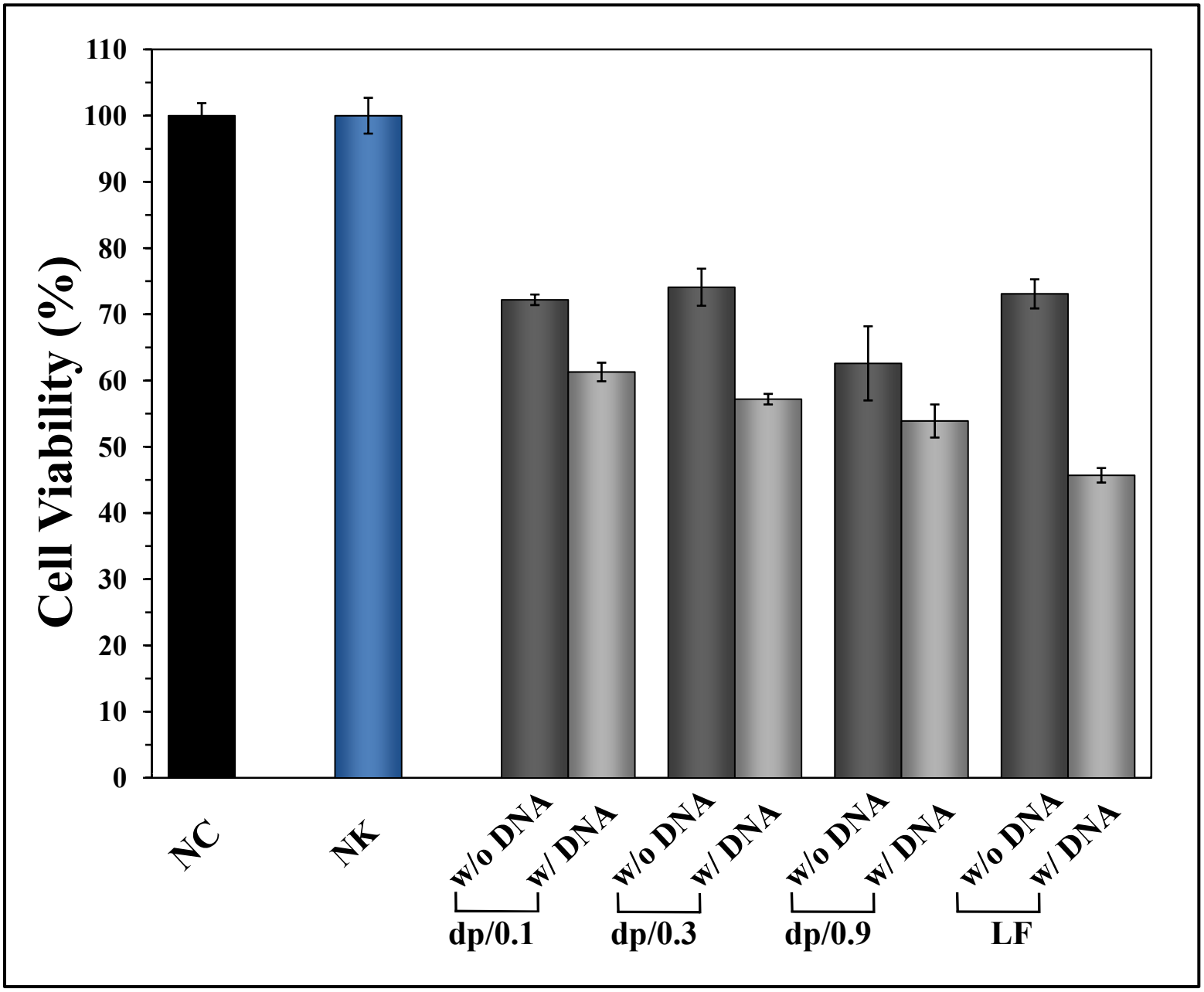
Cell Viability (%)
110
100
90
80
70
60
50
40
30
20
10
0
NC
NK
w/o DNA
w/ DNA
w/o DNA
w/ DNA
w/o DNA
w/ DNA
w/o DNA
w/ DNA
dp/0.1
dp/0.3
dp/0.9
LF

Figure 7

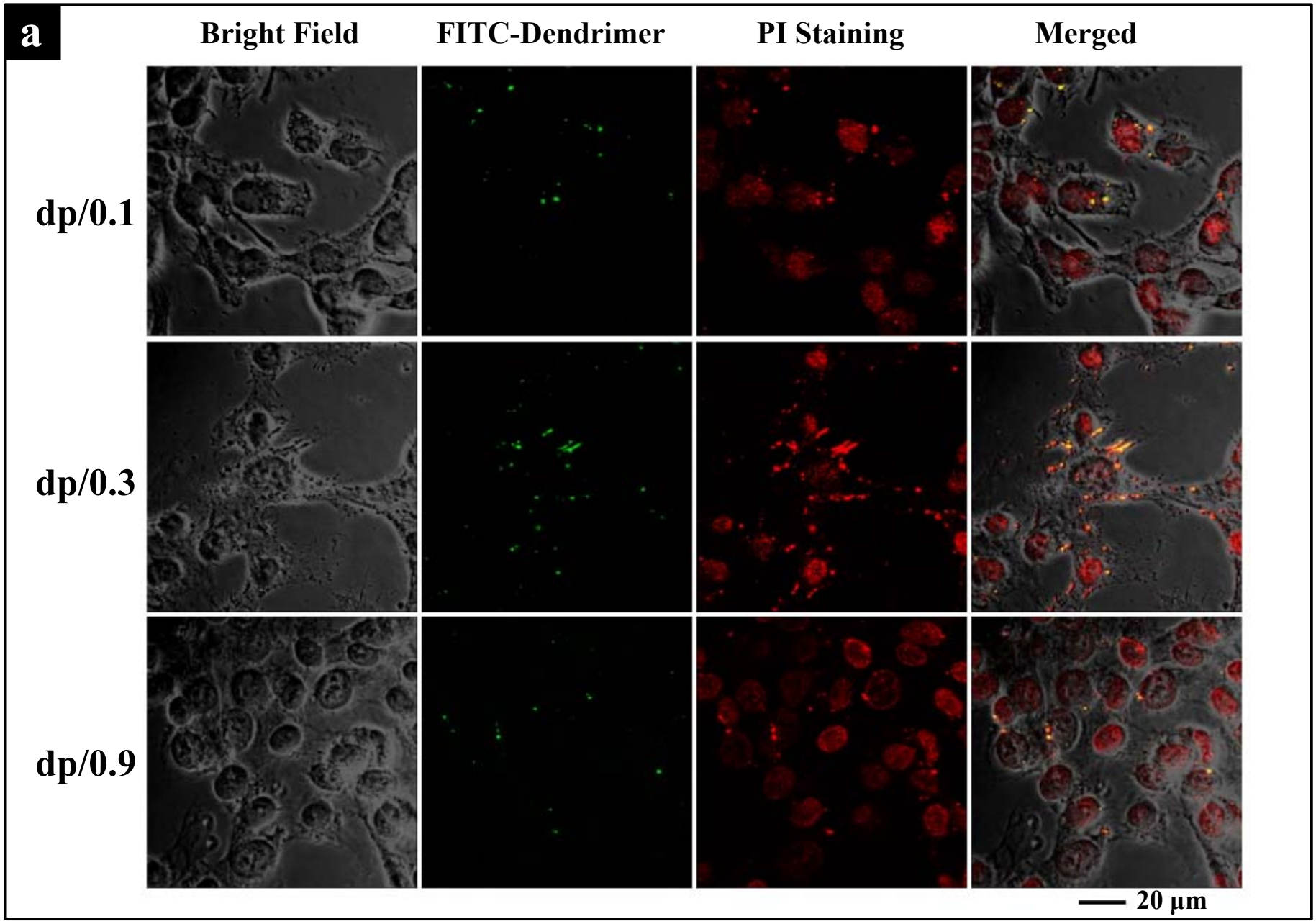
a
Bright Field
FITC-Dendrimer
PI Staining
Merged
dp/0.1
dp/0.3
dp/0.9
20 µm

Figure 7bcd

Figure 7

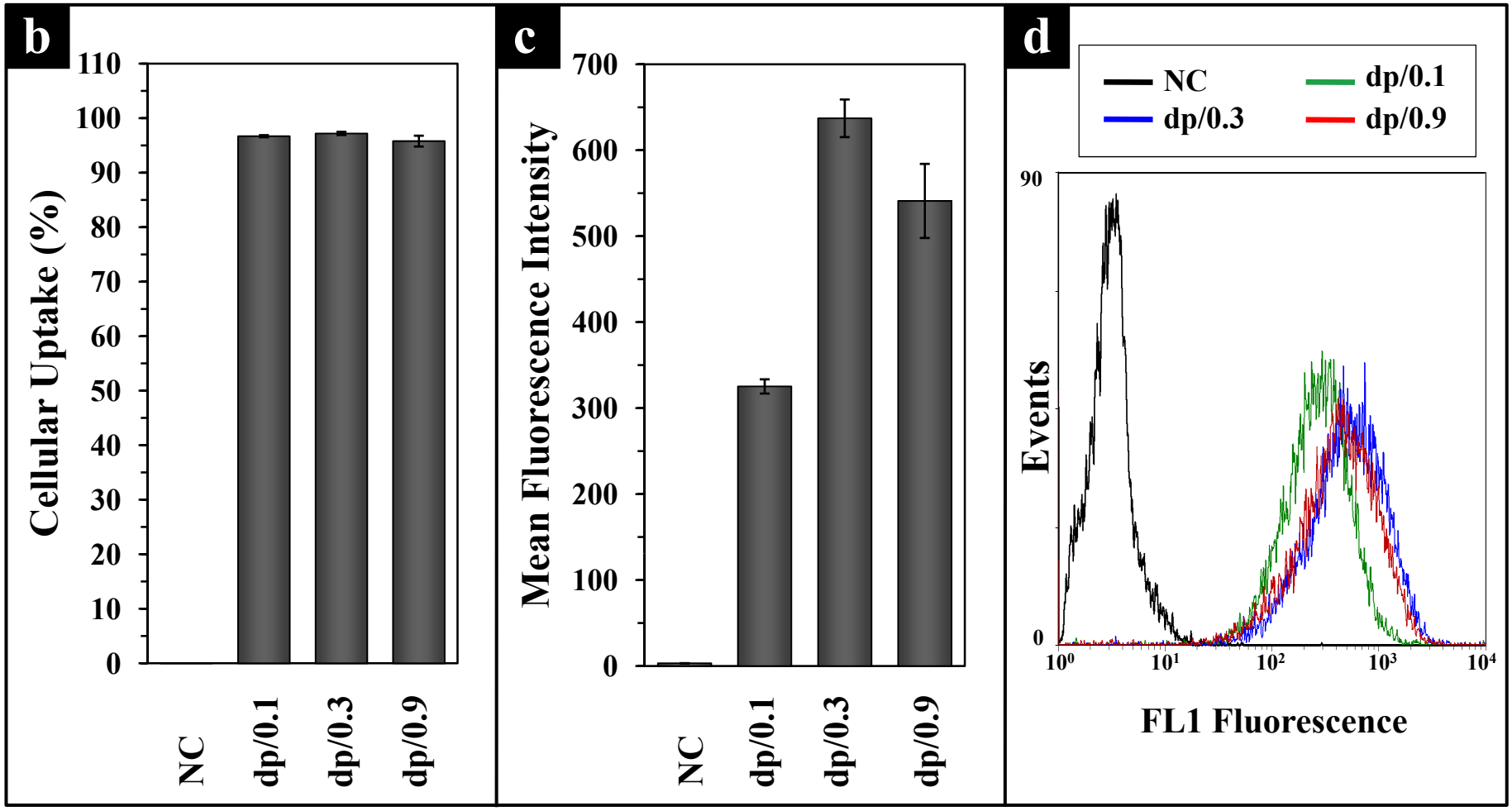

Figure 8

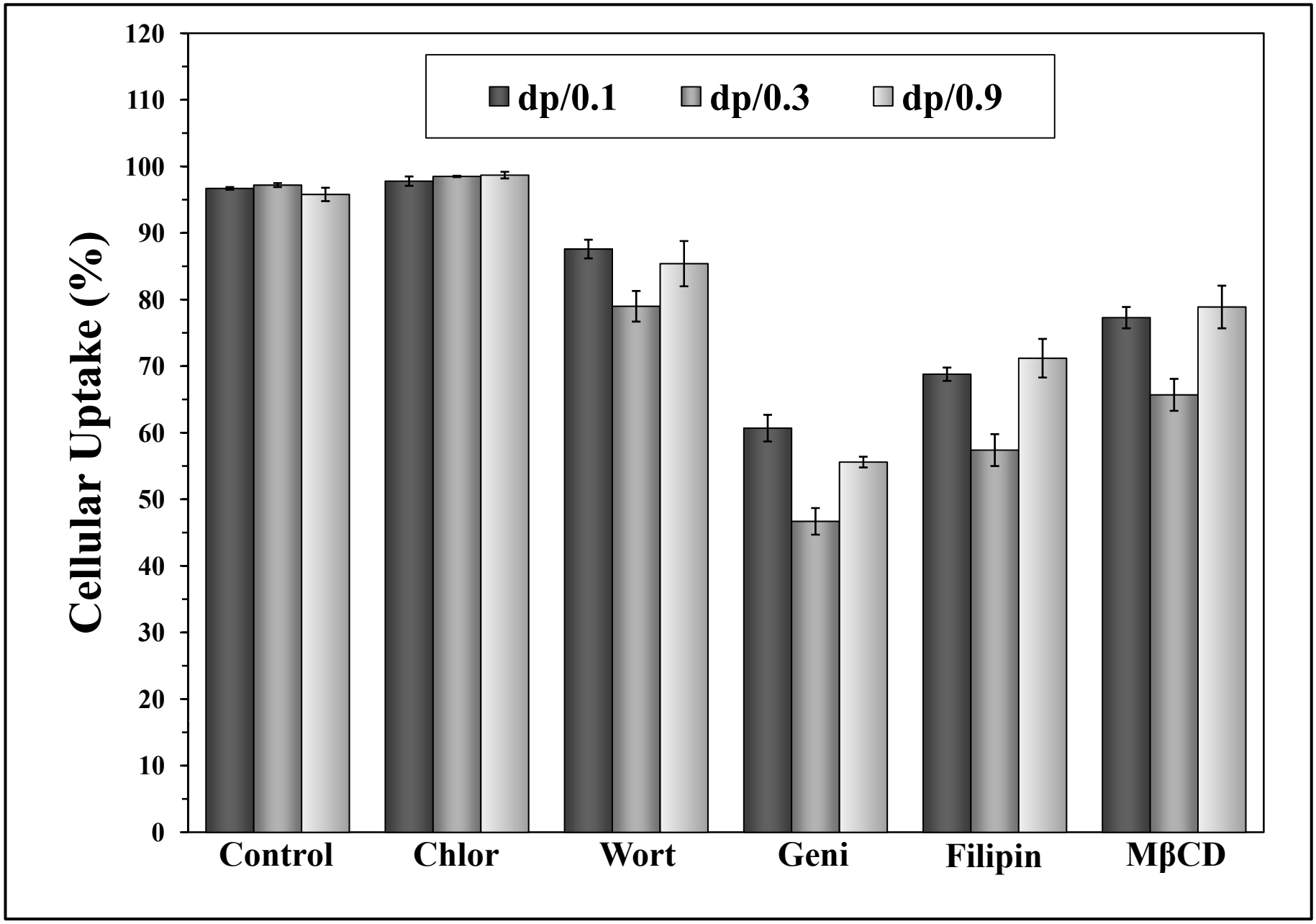
dp/0.1
dp/0.3
dp/0.9
Cellular Uptake (%)
120
110
100
90
80
70
60
50
40
30
20
10
0
Control
Chlor
Wort
Geni
Filipin
MβCD

Figure 9a

Figure 9

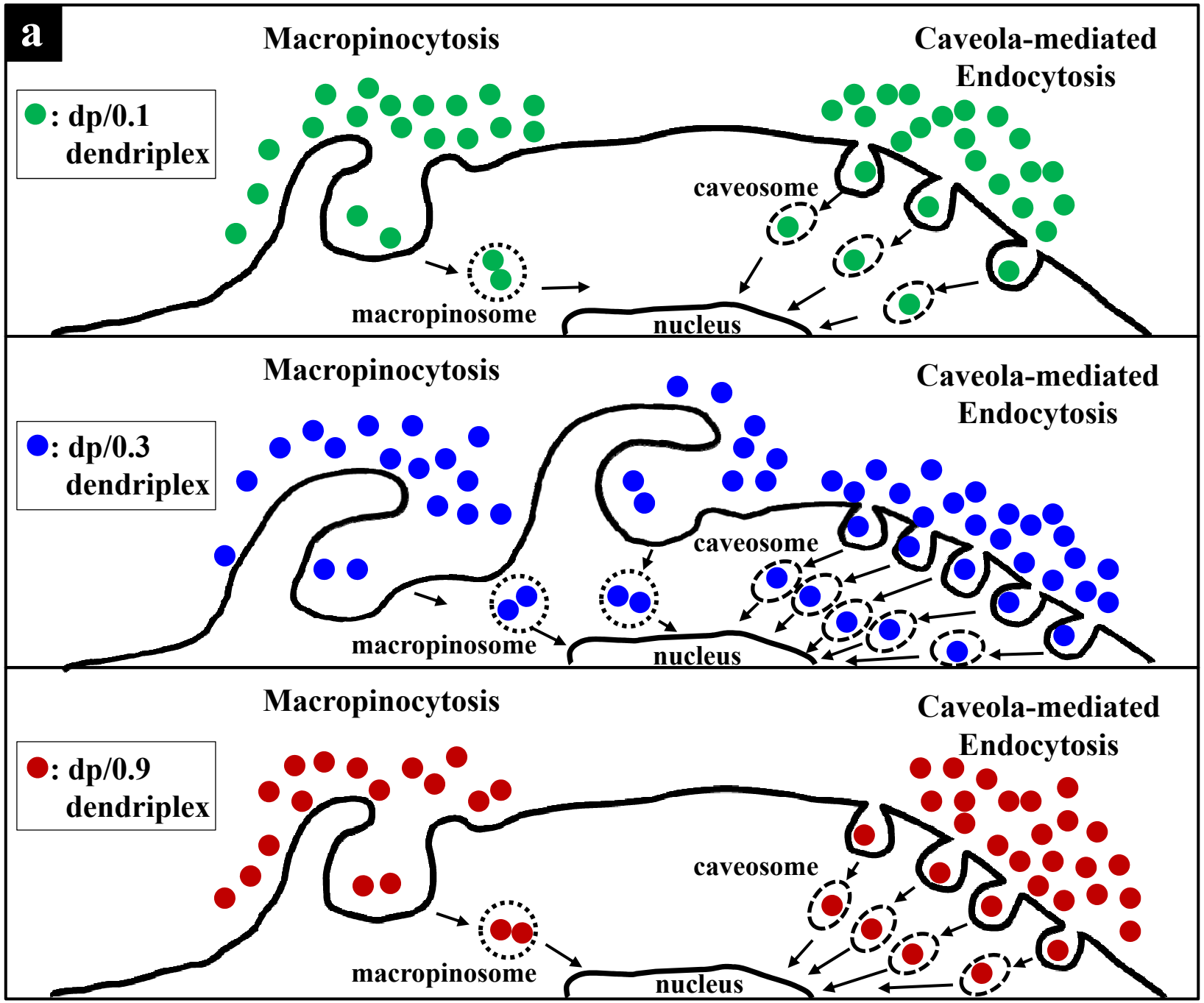

Figure 9

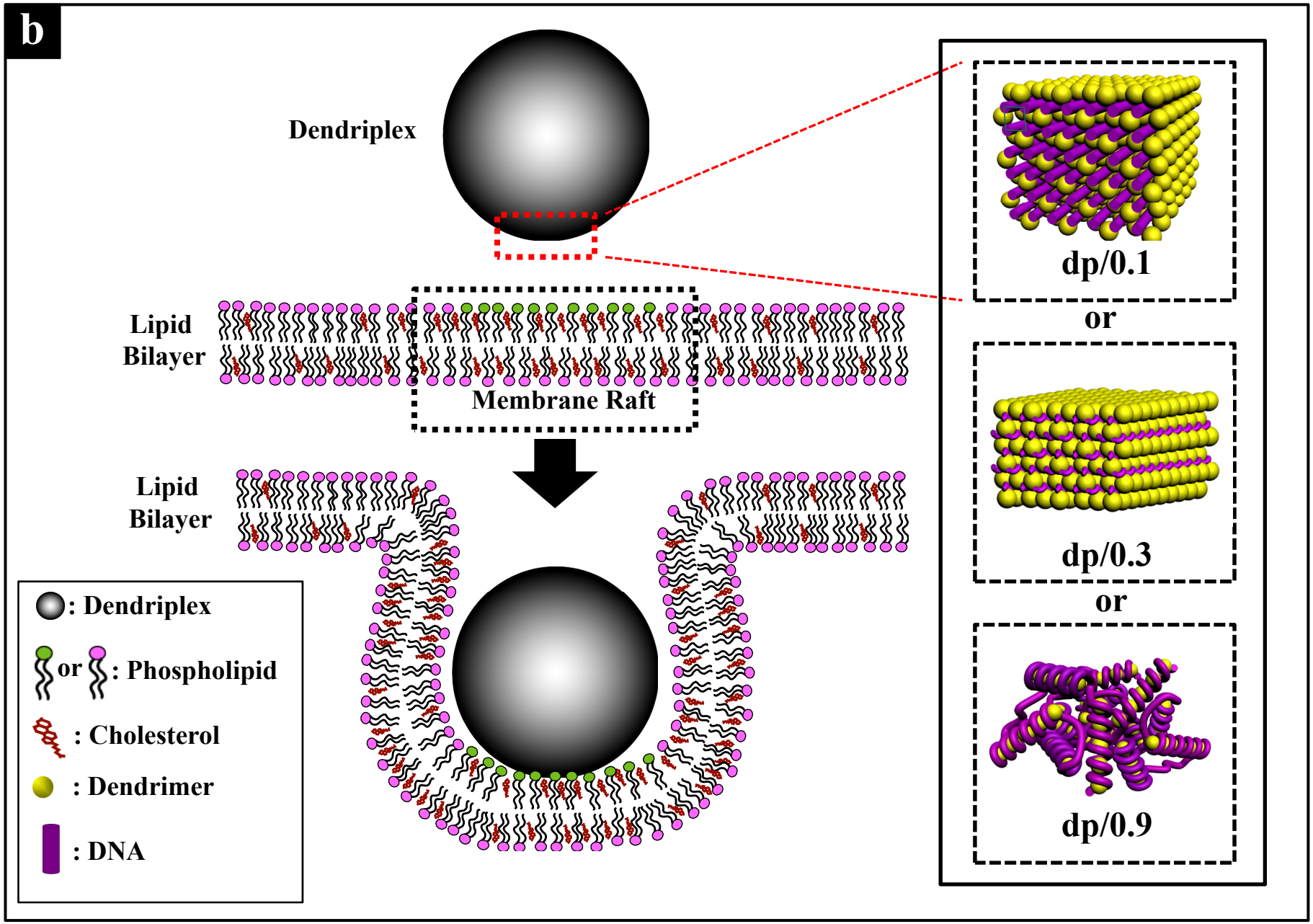
b
Dendriplex
Lipid Bilayer
Membrane Raft
Lipid Bilayer
: Dendriplex
or : Phospholipid
: Cholesterol
: Dendrimer
: DNA
dp/0.1
or
dp/0.3
or
dp/0.9